

# NUMERICAL SIMULATION OF A PLATE-GAP BIOSENSOR WITH AN OUTER POROUS MEMBRANE

**Feliksas Ivanauskas<sup>1,2</sup>, Romas Baronas<sup>1,2</sup>**

<sup>1</sup>Vilnius University, Faculty of Mathematics and Informatics

03225 Vilnius, Naugarduko 24, Lithuania

<sup>2</sup>Institute of Mathematics and Informatics

08663 Vilnius, Akademijos 4, Lithuania

*romas.baronas@mif.vu.lt(Romas Baronas)*

## Abstract

A plate-gap model of a porous enzyme doped electrode covered by a porous membrane has been proposed and analyzed. The two-dimensional-in-space mathematical model of the plate-gap biosensor is based on the reaction-diffusion equations containing a nonlinear term related to the Michaelis Menten kinetics of the enzymatic reaction. The developed model involves four regions: the enzyme layer where the enzymatic reaction as well as the mass transport by diffusion take place, the porous membrane as well as a diffusion limiting region where only a mass transport by diffusion takes place, and a convective region, where the analyte concentration is maintained constant. Assuming the porous membrane as the periodic media, the homogenization process was applied to the domain of the membrane and it was modelled as a homogeneous diffusion layer with an averaging diffusion coefficient. Using numerical simulation of the biosensor action, the influence of the geometry of the outer membrane on the biosensor response was investigated at wide range of analyte concentrations as well as of the reaction rates. The numerical simulation was carried out using the finite difference technique. The mathematical model as well as numerical solution were validated using analytical solutions existing for very specific cases of the model parameters. The behaviour of the plate-gap biosensor was compared with that of a flat electrode deposited with a layer of enzyme and covered with the same outer membrane.

**Keywords: Simulation, Modelling, Reaction-diffusion, Biosensor, Porous membrane.**

## Presenting Author's Biography

Feliksas Ivanauskas. He graduated from the Moscow State University in 1969, where he received his PhD in mathematics in 1974. In 1992 he received the Doctor Habilitus degree from the Institute of Mathematical Modelling, Russia. Now he is a professor (1992), a corresponding member of the Lithuanian Academy of Sciences, the head of the Department of Computer Science II at the Vilnius University and a principal researcher at the Department of Numerical Methods at the Institute of Mathematics and Informatics. His research interests are numerical methods for nonlinear PDE and mathematical modelling.



## 1 Introduction

Biosensors are sensing devices made up of a combination of a biological entity, usually an enzyme, that recognizes a specific analyte and the transducer that translates the biorecognition event into an electrical signal [1, 2]. The signal is proportional to the concentration of the analyte. The biosensors are classified according to the nature of the physical transducer. The amperometric biosensors measure the faradic current that arises on a working indicator electrode by direct electrochemical oxidation or reduction of the product of the biochemical reaction [2, 3].

The amperometric biosensors are known to be reliable, cheap and highly sensitive for environment, clinical and industrial purposes [4]. However, amperometric biosensors possess a number of serious drawbacks. One of the main reasons restricting wider use of the biosensors is a relatively short linear range of the calibration curve. Another serious drawback is the instability of bio-molecules. These problems can be partially solved by an application of an additional outer membrane on the surface of a biosensor [1, 2, 4]. Due to the technology of the biosensors preparation it is difficult to ensure the absolutely precise geometry of the electrodes as well as of the membranes. The sensitivity of the biosensor response to changes in the geometry of the biosensor is a new drawback.

Very recently a plate-gap model of a porous electrode was proposed and successfully applied to carbon paste based biosensors [5, 6, 7]. The plate-gap biosensors appear promising for detection of glucose, galactose, ethanol, phenol and some other substrates [8], particularly for phenol detection in waste water [9]. The purpose of this work was to enhance the mathematical model of the plate-gap biosensor with the external diffusion limiting region and to investigate the sensitivity of the biosensor response to changes in the geometry of the gaps as well as of the porous membrane. The model is based on reaction-diffusion equations containing a non-linear term related to Michaelis-Menten kinetics of the enzymatic reaction. The developed model involves four regions: the enzyme layer where enzyme reaction as well as the mass transport by diffusion take place, the porous membrane as well as a diffusion limiting region where only the mass transport by diffusion takes place, and a convective region, where the analyte concentration is maintained constant.

The simulation of the biosensor response was carried out using the finite difference technique [10]. The mathematical model as well as the numerical solution were validated using analytical solutions existing for very specific cases of the model parameters. The simulation results were also compared with similar experimental studies [5]. A satisfactory agreement between the numerical solution and experimental data has been obtained.

## 2 Principal structure of a biosensor

Fig. 1 shows a principal structure of a biosensor, where enzyme filled gaps are modelled by right quadrangular prisms of base  $2a_1$  by  $c$  distributed uniformly so, that the distance between adjacent prisms equals to  $2(a_2 - a_1)$ ,  $a_1$  is the half width of the gaps,  $c$  is the gap depth and  $d$  is the thickness of the porous membrane.

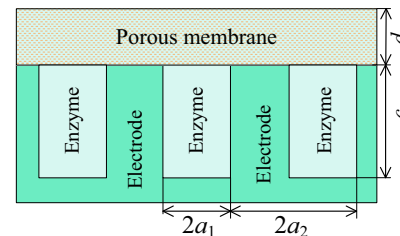


Fig. 1 A principal structure of a plate-gap biosensor

We assume that the thickness of the outer membrane as well as the depth of the gaps of the electrode are much less than its length. The porous membrane is assumed of a uniform thickness. Due to the uniform distribution of the gaps, it is reasonable to consider only a unit consisting of a single gap together with the region between two adjacent gaps. Because of the symmetry and the relatively great length of the gaps we consider only the transverse section of a half of the unit.

Fig. 2 shows the profile of a unit cell to be considered in mathematical modelling of the biochemical behaviour of the plate-gap biosensor.

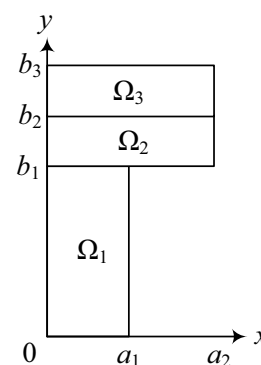


Fig. 2 A profile of the unit cell of the plate-gap biosensor

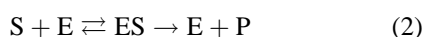
In Fig. 2,  $\Omega_1$  represents the enzyme-filled gaps,  $\Omega_2$  corresponds to the porous membrane and  $\Omega_3$  stands for the external diffusion layer.  $c = b_1$  is the depth of the gaps,  $d = b_2 - b_1$  is the thickness of the porous membrane and  $\delta = b_3 - b_2$  is the thickness of the external diffusion layer. A very similar approach has been used in modelling of partially blocked electrodes [11, 12] as well as in modelling of biosensors with perforated and selective membranes [13].

### 3 Mathematical model

The mathematical model of a plate-gap biosensor with an outer porous membrane (Figs. 1 and 2) may be formulated in a two dimensional domain consisting mainly of three regions: the enzyme region  $\Omega_1$ , the region  $\Omega_2$  corresponding to the porous membrane and the region  $\Omega_3$  of the external diffusion,

$$\begin{aligned}\Omega_1 &= (0, a_1) \times (0, b_1), \\ \Omega_2 &= (0, a_2) \times (b_1, b_2), \\ \Omega_3 &= (0, a_2) \times (b_2, b_3).\end{aligned}\quad (1)$$

In the enzyme region  $\Omega_1$  we consider the mass transport by diffusion and the enzyme-catalysed reaction



In this scheme the substrate (S) combines reversibly with an enzyme (E) to form a complex (ES). The complex then dissociates into a product (P) and the enzyme is regenerated. Assuming the quasi steady state approximation, the concentration of the intermediate complex (ES) do not change and may be neglected when simulating the biochemical behaviour of biosensors [1, 2].

Assuming the porous membrane as the periodic media, the homogenization process has been applied to the domain  $\Omega_2$  of the membrane [14]. After this, the porous membrane was modelled as a diffusion layer with an averaging diffusion coefficient.

In the homogeneous external region  $\Omega_3$  also only the mass transport by diffusion of the substrate as well as of the product takes place.

The thickness  $\delta$  of the diffusion layer depends upon the nature and intensity of flowing or stirring of the buffer solution [15].  $\delta$  is inversely proportional to the intensity of the stirring (e.g. rotation speed of the electrode). That diffusion layer is known as the Nernst layer. The thickness of the Nernst diffusion layer practically does not depend upon the outer membrane thickness. In practice, the zero thickness of the Nernst layer can not be achieved [16]. That thickness may be minimized only up to  $\delta = 2 \mu\text{m}$  by increasing the intensity of stirring or flowing of the buffer solution [16].

#### 3.1 Governing equations

The action of the biosensor, presented schematically in Figs. 1 and 2, can be described by the following reaction-diffusion system ( $t > 0$ ) [17]:

$$\frac{\partial S_1}{\partial t} = D_1 \Delta S_1 - \frac{V_{max} S_1}{K_M + S_1}, \quad (3)$$

$$\frac{\partial P_1}{\partial t} = D_1 \Delta P_1 + \frac{V_{max} S_1}{K_M + S_1}, \quad (x, y) \in \Omega_1,$$

$$\frac{\partial S_j}{\partial t} = D_j \Delta S_j, \quad (4)$$

$$\frac{\partial P_j}{\partial t} = D_j \Delta P_j, \quad (x, y) \in \Omega_j, \quad j = 2, 3,$$

where  $\Delta$  is the Laplacian,  $S_i(x, y, t)$  is the concentration of the substrate in  $\Omega_i$ ,  $P_i(x, y, t)$  is the concentration of the reaction product in  $\Omega_i$ ,  $i = 1, 2, 3$ ,  $V_{max}$  is the maximal enzymatic rate and  $K_M$  is the Michaelis constant.

#### 3.2 Initial conditions

Let  $\bar{\Omega}_i$  be the closure of the corresponding open region  $\Omega_i$ ,  $i = 1, 2, 3$ ,  $\Gamma_1$  - the electrode surface and  $\Gamma_2$  - the porous membrane/bulk solution boundary,

$$\begin{aligned}\Gamma_1 &= ([0, a_1] \times \{0\}) \cup (\{a_1\} \times [0, b_1]) \cup \\ &\quad ([a_1, a_2] \times \{b_1\}), \\ \Gamma_2 &= [0, a_2] \times \{b_3\}.\end{aligned}\quad (5)$$

The biosensor operation starts when the substrate of concentration  $S_0$  appears in the bulk solution. This is used in the initial conditions ( $t = 0$ ) [17]:

$$\begin{aligned}S_k(x, y, 0) &= 0, \quad (x, y) \in \bar{\Omega}_k, \quad k = 1, 2, \\ S_3(x, y, 0) &= 0, \quad (x, y) \in \bar{\Omega}_3 \setminus \Gamma_2, \\ S_3(x, y, 0) &= S_0, \quad (x, y) \in \Gamma_2, \\ P_i(x, y, 0) &= 0, \quad (x, y) \in \bar{\Omega}_i, \quad i = 1, 2, 3.\end{aligned}\quad (6)$$

#### 3.3 Boundary and matching conditions

Assuming  $b_0 = 0$ , the following boundary conditions express the symmetry of the biosensor:

$$\begin{aligned}\frac{\partial P_i}{\partial x} \Big|_{x=0} &= \frac{\partial S_i}{\partial x} \Big|_{x=0} = 0, \quad y \in [b_{i-1}, b_i], \\ \frac{\partial P_j}{\partial x} \Big|_{x=a_2} &= \frac{\partial S_j}{\partial x} \Big|_{x=a_2} = 0, \quad y \in [b_{j-1}, b_j], \\ t > 0, \quad i &= 1, 2, 3, \quad j = 2, 3.\end{aligned}\quad (7)$$

The following boundary condition on the electrode border  $\Gamma_1$  defines the electrochemical process ( $k = 1, 2$ ):

$$\begin{aligned}\frac{\partial S_k}{\partial n} \Big|_{\Gamma_1} &= 0, \quad P_k = 0, \\ (x, y) &\in \Gamma_1, \quad k = 1, 2,\end{aligned}\quad (8)$$

where  $n$  stands for the normal direction.

If the bulk solution is well-stirred and in powerful motion then the diffusion layer ( $b_2 < y < b_3$ ) may be treated as the Nernst diffusion layer [11, 15]. According to the Nernst approach, a layer of thickness  $\delta = b_3 - b_2$  remains unchanged with time. Away from it, the solution is in motion and is uniform in concentration ( $t > 0$ ),

$$\begin{aligned}S_3(x, b_3, 0) &= S_0, \\ P_3(x, b_3, 0) &= 0, \quad x \in [0, a_2].\end{aligned}\quad (9)$$

On the boundary between adjacent regions  $\Omega_k$  and

$\Omega_{k+1}$  we define the matching conditions,

$$\begin{aligned} D_k \frac{\partial S_k}{\partial y} \Big|_{y=b_k} &= D_{k+1} \frac{\partial S_{k+1}}{\partial y} \Big|_{y=b_k}, \\ S_k(x, b_k, t) &= S_{k+1}(x, b_k, t), \\ D_k \frac{\partial P_k}{\partial y} \Big|_{y=b_k} &= D_{k+1} \frac{\partial P_{k+1}}{\partial y} \Big|_{y=b_k}, \\ P_k(x, b_k, t) &= P_{k+1}(x, b_k, t), \\ (x, y) &\in \bar{\Omega}_k \cap \bar{\Omega}_{k+1}, \quad t > 0, \quad k = 1, 2. \end{aligned} \quad (10)$$

The governing Eqs. (3), (4) together with the initial (6), boundary (7)-(9) and matching (10) conditions form together a boundary value problem.

### 3.4 Characteristics of the biosensor response

The measured current is accepted as a response of a biosensor in an actual experiment. The current depends upon the flux of the reaction product at the electrode surface, i.e. on the border  $\Gamma_1$ . The density  $i(t)$  of the current at time  $t$  can be obtained explicitly from the Faraday's and Fick's laws

$$\begin{aligned} i(t) &= \frac{n_e F}{a_2} \left( D_1 \int_0^{a_1} \frac{\partial P_1}{\partial y} \Big|_{y=0} dx + \right. \\ &D_1 \int_0^{b_1} \frac{\partial P_1}{\partial x} \Big|_{x=a_1} dy + \\ &\left. D_2 \int_{a_1}^{a_2} \frac{\partial P_2}{\partial y} \Big|_{y=b_1} dx \right), \end{aligned} \quad (11)$$

where  $n_e$  is a number of electrons involved in a charge transfer and  $F$  is the Faraday constant. We assume, that the system (3)-(10) approaches steady state when  $t \rightarrow \infty$ ,

$$I = \lim_{t \rightarrow \infty} i(t), \quad (12)$$

where  $I$  is the steady state current of the plate-gap biosensor.

## 4 Numerical simulation

Analytical solutions are not usually possible when analytically solving multi-dimensional nonlinear partial differential equations in a domain of the complex geometry [15, 18]. Therefore, the problem was solved numerically using the finite difference technique [10]. To find a numerical solution of the problem we introduced a bilinear discrete grid in all the directions:  $x$ ,  $y$  and  $t$  [7, 13, 19]. Using alternating direction method a semi-implicit linear finite difference scheme has been built as a result of the difference approximation [10]. The resulting system of linear algebraic equations was solved rather efficiently because of the tridiagonality of the matrix of the system.

Due to high gradients of the concentrations of both species: substrate and product, an accurate and stable numerical solution was achieved only at very small step size in  $y$  direction at the boundaries  $y = 0$  and  $y = b_3$ . Because of the concavity of an angle at point  $(a_1, b_1)$  it was necessary to use very small step size in both space

directions:  $x$  and  $y$  also at the boundaries  $x = a_1$ ,  $y = b_1$ . Due to the matching conditions between adjacent regions with different diffusivities, we used also small step size at the boundary  $y = b_2$ . We assumed, that farther from all these peculiar boundaries, step size may increase in both space directions:  $x$  and  $y$ . Consequently, in the direction  $x$ , an exponentially increasing step size was used to both sides from  $a_1$ : to  $a_2$  and down to 0. In the direction  $y$ , an exponentially increasing step size was used from 0 to  $b_1/2$ , from  $b_3$  down to  $(b_2 + b_3)/2$ , from  $b_j$  down to  $(b_j + b_{j-1})/2$  and from  $b_j$  to  $(b_j + b_{j+1})/2$ ,  $j = 1, 2$ , where  $b_0 = 0$ .

The step size in the direction of time was restricted due to the nonlinear reaction term in Eq. (3), boundary conditions and the geometry of the domain. In order to achieve accurate and stable solution of the problem, at the beginning of the reaction-diffusion process we employed the restrictive condition, which is usually used for fully explicit schemes. Since the biosensor action obeys the steady state assumption when  $t \rightarrow \infty$ , it was reasonable to apply an increasing step size in the time direction. The final step size was in a few orders of magnitude higher than the first one. The digital simulator has been programmed in JAVA language [20].

In digital simulation, the biosensor response (steady state) time was assumed as the time when the absolute current slope value falls below a given small value normalized with the current value [13, 17]. In other words, the time  $T_R$  needed to achieve a given dimensionless decay rate  $\varepsilon$  was used

$$T_R = \min_{i(t) > 0} \left\{ t : \frac{1}{i(t)} \left| \frac{di(t)}{dt} \right| \right\}, \quad i(T_R) \approx I. \quad (13)$$

In calculations, we used  $\varepsilon = 10^{-5}$ .

Assuming  $a_1 = a_2 \gg b_1$  and the zero thickness either of the porous membrane or of the external diffusion layer ( $d = 0$  or  $\delta = 0$ ), the mathematical model (3)-(10) approaches to a two-compartment mathematical model of a flat two-layer amperometric biosensor [17]. At relatively low ( $S_0 \ll K_M$ ) as well as at very high ( $S_0 \gg K_M$ ) concentrations of the substrate  $S_0$ , the two-compartment mathematical model can be solved analytically [17].

The adequacy of the mathematical model (3)-(10) of the plate-gap biosensor as well as of the numerical solution of that problem were evaluated using known analytical solutions of the two-compartment mathematical model [17]. Accepting  $a_1 = a_2 = 20b_1$ , the steady state biosensor current was calculated at different values of the model parameters: maximal enzymatic rate  $V_{max}$ , the substrate concentration  $S_0$  ( $S_0 \ll K_M$  as well as  $S_0 \gg K_M$ ), the gap depth  $c = b_1$ , the thickness  $d$  of the outer membrane (accepting  $\delta = 0$ ) and the thickness  $\delta$  of the external diffusion layer (accepting  $d = 0$ ). In all the cases the relative difference between the numerical and analytical solutions was less than 1%.

Results of the numerical simulation obtained for the plate-gap biosensor were also compared with similar experimental studies [5]. A satisfactory agreement be-

tween the numerical solution and experimental data has been obtained.

Fig. 3 shows the simulated dynamics of the biosensor current at different values of the maximal enzymatic rate  $V_{max}$  and the substrate concentration  $S_0$ .

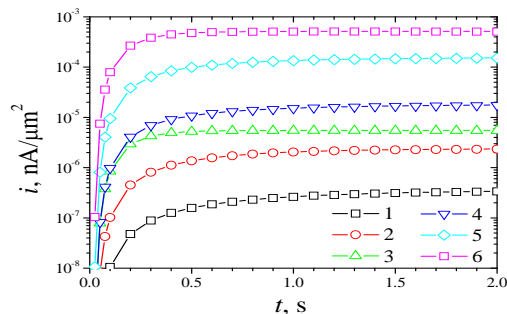


Fig. 3 The dynamics of the biosensor current  $i(t)$ ,  $S_0$ : 0.01 (1-3), 1 (4-6) (mM),  $V_{max}$ : 0.1 (1, 4), 1 (2, 5), 10 (3, 6) (mM/s),  $a_1 = 1$ ,  $a_2 = a_1 + 1$ ,  $b_1 = 4$ ,  $b_2 = b_1 + 2$ ,  $b_3 = b_2 + 2$  ( $\mu\text{m}$ ),  $D_1 = 100$ ,  $D_2 = 10$ ,  $D_3 = 2D_1$  ( $\mu\text{m}^2/\text{s}$ ),  $K_M = 1$  (mM)

As one can see in Fig. 3 that the biosensor current is very sensitive to changes of  $V_{max}$  and  $S_0$ . Changing values of these two parameters, the steady state current varies even in orders of magnitude. This is a rather ordinary feature of amperometric biosensors [1, 7].

## 5 Results of calculations

Using numerical simulation, the influence of changes in the geometry of the gaps as well as of the porous membrane on the biosensor response was investigated.

The steady state biosensor current was calculated at different values of the maximal enzymatic rate  $V_{max}$  and substrate concentration  $S_0$ . Because of the high sensitivity of the biosensor current to changes of  $V_{max}$  and  $S_0$  (Fig. 3) we normalized the biosensor current.

### 5.1 The effect of the geometry of gaps

In the model of the plate-gap biosensor (Figs. 1 and 2), the parameter  $c$  ( $c = b_1$ ) stands for the depth of the gaps in the electrode. Fig. 4 shows the dependence of the steady state biosensor current on the depth  $c$ . The biosensor responses were calculated at constant thickness  $d = 2 \mu\text{m}$  of the porous membrane, constant thickness  $\delta = 2 \mu\text{m}$  of the external diffusion layer changing  $c$  from 2 to  $6 \mu\text{m}$ . In this case the steady state current was normalized with respect to the minimal value  $c_0$  of  $c$  to be analyzed,

$$I_c(c) = \frac{I(c)}{I(c_0)}, \quad (14)$$

where  $I_c(c)$  is the steady state biosensor current calculated at given depth  $c$  of the gaps,  $c_0 = 2 \mu\text{m}$ .

As it is possible to notice in Fig. 4, the steady state current of the plate-gap biosensor is a monotonous increasing function of  $c$ . However,  $I_c$  is practically constant functions of  $c$  at high maximal enzymatic rate  $V_{max}$  (10 mM/s, curves 3 and 6).

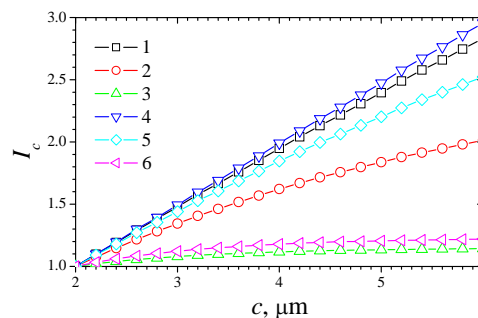


Fig. 4 The normalized steady state current  $I_c$  versus the gap depth  $c = b_1$ , other parameters and notations are the same as in Fig. 3

To investigate the dependence of the biosensor response on the width of the gaps we calculated the biosensor response at a constant distance  $2(a_2 - a_1)$  between two adjacent gaps changing the half width  $a_1$  from 0.5 to  $5.5 \mu\text{m}$ . As it was mentioned above, increasing the half width  $a_1$  of the gaps the current of the plate-gap biosensor approaches the current of the corresponding flat one. Because of this the steady state current of the plate-gap biosensor was normalized with the steady state current of the corresponding flat biosensor,

$$I_a(a) = \frac{I(a)}{I(\infty)}, \quad (15)$$

where  $I(a)$  is the steady state current calculated assuming the half width  $a$  of the gaps,  $I(\infty)$  is the steady state of the corresponding flat biosensor.

Fig. 5 shows the dependence of the steady state current of the plat-gap biosensor on the width of the gaps at different values of  $V_{max}$  and  $S_0$ . At very high maximal enzymatic rate  $V_{max}$  (10 mM/s) (curves 3 and 6)  $I(a)$  approaches  $I(\infty)$  notable faster than at other values of  $V_{max}$ . The effect of the substrate concentration  $S_0$  is fairly low.

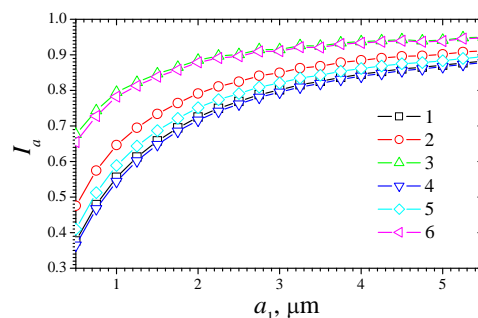


Fig. 5 The normalized steady state current  $I_a$  versus the width  $a_1$  of gaps, other parameters and notations are the same as in Fig. 3

An increase in the width as well as in the depth of the gaps increases the total volume of the enzyme used in plate gap biosensors. Fig. 6 shows the dependence of the steady state current on the distance between the gaps. The total volume of the enzyme decreases with

increase in the distance  $a_2$ . Summarizing the results presented in Figs. 4, 5 and 6, we can conclude, that the plate-gap biosensor is more resistant to changes in volume of the enzyme at higher values of  $V_{max}$  rather than at lower ones.

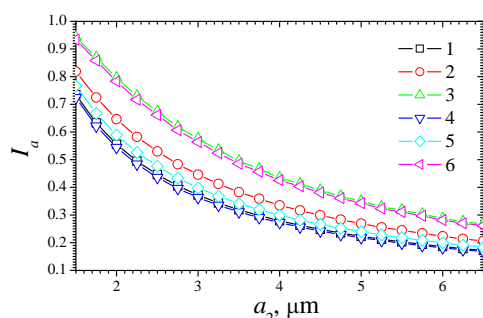


Fig. 6 The normalized steady state current  $I_a$  versus the half distance  $a_2$  between centers of adjacent gaps, other parameters and notations are the same as in Fig. 3

## 5.2 The effect of the porous membrane

Using numerical simulation, the influence of the thickness and of the permeability (porosity) of the outer porous membrane on the biosensor current was investigated. In terms of the mathematical model (3)-(10), the permeability as well as the porosity is expressed by the diffusion coefficient  $D_2$ .

To investigate the effect of the thickness  $d$  of the membrane on the biosensor response, the steady state current of the biosensor having the outer membrane was normalized with the steady state current of the corresponding biosensor having no outer membrane,

$$I_d(d) = \frac{I(d)}{I(0)}, \quad (16)$$

where  $I(d)$  is the steady state biosensor current calculated at given thickness  $d$  of the outer membrane.

Fig. 7 shows the dependence of the steady state biosensor current on the thickness  $d$  of the outer porous membrane.

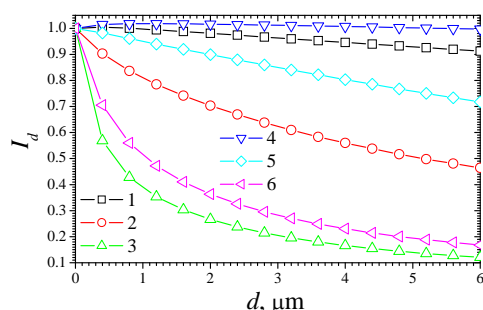


Fig. 7 The normalized steady state current  $I_d$  versus the the thickness  $d$  of the porous membrane, other parameters and notations are the same as in Fig. 3

One can see in Fig. 7, that the normalized steady state current  $I$  (as well as the non-normalized one  $I_d$ )

is a monotonous decreasing function of the thickness  $d$  at relatively high values of the enzymatic activity ( $V_{max} \geq 1$  mM/s).  $I_d$  is a slightly non-monotonous function of  $d$  at low value of  $V_{max}$  (0.1 mM/s, curves 1 and 4). Fig. 7 shows, that the plate-gap biosensor is more resistant to changes in the thickness of the outer membrane at lower values of  $V_{max}$  rather than at higher ones.

The maximal enzymatic rate  $V_{max}$  actually is a product of two parameters: the catalytical constant  $K_{cat}$  and the total concentration  $E_t$  of the enzyme [1, 2]. In real applications of biosensors it usually is impossible to modify the  $K_{cat}$  part. The maximal rate  $V_{max}$  might be modified by changing the concentration  $E_t$  of the enzyme in the enzyme layer.  $V_{max}$  is relative to total enzyme used in a biosensor.

To investigate the dependence of the biosensor response on the diffusivity  $D_2$  of the outer porous membrane, the current was normalized with respect to the diffusivity  $D_1$  of the species in the enzyme,

$$I_D(D) = \frac{I(D)}{I(D_1)}, \quad (17)$$

where  $I(D)$  is the steady state biosensor current calculated at given diffusivity  $D$  of the species in the outer membrane. Results of the calculations are depicted in Fig. 8, where one can see, that the effect of the diffusivity  $D_2$  notably depends on the maximal enzymatic rate  $V_{max}$ .

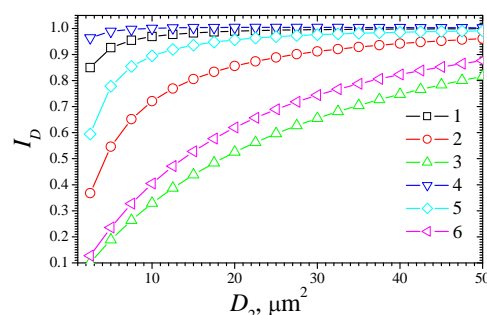


Fig. 8 The normalized steady state current  $I_D$  versus the diffusivity  $D_2$  of the porous membrane, other parameters and notations are the same as in Fig. 3

Although the shapes of curves in Fig. 8 notable differ from those in Fig. 7, the effect of the diffusivity  $D_2$  of the membrane is very similar to that of the membrane thickness  $d$ . A decrease in diffusivity  $D_2$  influences the steady state current similarly to the increase in thickness  $d$  of the membrane. To show the similarities more apparent, the normalized steady state current  $I_d$  (Fig. 7) was replotted in Fig. 9 as a function of the inverse thickness  $1/d$  of the outer membrane. The shapes of curves in Fig. 9 are approximately the same as in Fig. 8.

## 6 Concluding remarks

The mathematical model (3)-(10) of the operation of the amperometric plate-gap biosensor with an outer porous

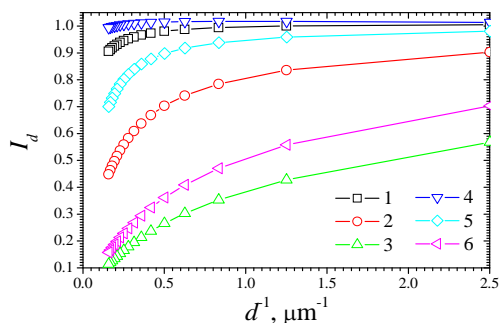


Fig. 9 The normalized steady state current  $I_d$  versus the the inverse thickness  $d^{-1}$  of the porous membrane, other parameters and notations are the same as in Fig. 3

membrane can be used to investigate peculiarities of the biosensor response in stirred and non stirred analytes.

At high maximal enzymatic rates  $V_{max}$  the response of the plate-gap biosensor is more resistant to changes in the geometry of the enzyme-filled gaps rather than at lower values of  $V_{max}$  (Figs. 4, 5 and 6). This feature of the biosensor response can be applied in design of novel highly sensitive biosensors when the minimization of the enzyme volume is of crucial importance. Selecting the geometry of gaps allows minimizing the volume of enzyme without loosing the sensitivity.

The response of the plate-gap biosensor is more resistant to changes in the thickness  $d$  as well as in the diffusivity  $D_2$  of the outer membrane at lower values of  $V_{max}$  rather than at higher ones (Figs. 7, 8 and 9). It is very important to take this feature into account when designing long-term operating analytical systems in which the activity of the enzyme ( $V_{max}$ ) permanently decreases.

## Acknowledgement

The authors express sincere gratitude to prof. Juozas Kulys and prof. Valdas Laurinavičius for their valuable contribution to modelling of biosensors.

## 7 References

- [1] F. Scheller and F. Schubert. *Biosensors*. Elsevier, Amsterdam, 1992.
- [2] A.P.F. Turner, I. Karube, and G.S. Wilson. *Biosensors: Fundamentals and Applications*. Oxford University Press, Oxford, 1987.
- [3] A. Chaubey and B.D. Malhotra. Mediated biosensors. *Biosensors and Bioelectronics*, 17:441–456, 2002.
- [4] U. Wollenberger, F. Lisdat, and F.W. Scheller. *Frontiers in Biosensorics 2. Practical Applications*. Birkhauser Verlag, Basel, 1997.
- [5] V. Laurinavicius, J. Razumiene, A. Ramanavicius, and A.D. Ryabov. Wiring of PQQ-dehydrogenases. *Biosensors and Bioelectronics*, 20:1217–1222, 2004.
- [6] F. Ivanauskas, I. Kaunietis, V. Laurinavicius, J. Razumiene, and R. Simkus. Computer simulation

of the steady state currents at enzyme doped carbon paste electrode. *Journal of Mathematical Chemistry*, 38:355–366, 2005.

- [7] R. Baronas, F. Ivanauskas, I. Kaunietis, and V. Laurinavicius. Mathematical modeling of plate-gap biosensors with an outer porous membrane. *Sensors*, 6:727–745, 2006.
- [8] V. Laurinavicius, J. Razumiene, B. Kurtinaitiene, I. Lapenaite, I. Bachmatova, L. Marcinkeviciene, R. Meskys, and A. Ramanavicius. Bioelectrochemical application of some PQQ-dependent enzymes. *Bioelectrochemistry*, 55:29–32, 2002.
- [9] INTELLISENS. *Intelligent Signal Processing of Biosensor Arrays Using Pattern Recognition for Characterisation of Wastewater: Aiming Towards Alarm Systems*. EC RTD project, 2000–2003.
- [10] A.A. Samarskii. *The Theory of Difference Schemes*. Marcel Dekker, New York-Basel, 2001.
- [11] C. Deslous, C. Gabrielli, M. Keddam, A. Khalil, R. Rosset, B. Tribollet, and M. Zidoune. Impedance techniques at partially blocked electrodes by scale deposition, *Electrochimica Acta*, 42:1219–1233, 1997.
- [12] R. Baronas, F. Ivanauskas, and A. Survila. Simulation of electrochemical behavior of partially blocked electrodes under linear potential sweep conditions. *Journal of Mathematical Chemistry*, 27:267–278, 2000.
- [13] R. Baronas, J. Kulys, and F. Ivanauskas. Computational modelling of biosensors with perforated and selective membranes. *Journal of Mathematical Chemistry*, 39:345–362, 2006.
- [14] N.S. Bakhvalov and G.P. Panasenko. *Homogenization: Averaging Processes in Periodic Media*. Kluwer Academic Publishers, Dordrecht, 1989.
- [15] D. Britz. *Digital Simulation in Electrochemistry*. Springer-Verlag, Berlin, 2005.
- [16] J. Wang. *Analytical Electrochemistry*. John Wiley & Sons, New-York, 2000.
- [17] T. Schulmeister. Mathematical modeling of the dynamic behaviour of amperometric enzyme electrodes. *Selective Electrode Review*, 12:203–260, 1990.
- [18] L.K. Bieniasz and D. Britz. Recent developments in digital simulation of electroanalytical experiments. *Polish Journal of Chemistry*, 78:1195–1219, 2004.
- [19] R. Baronas, F. Ivanauskas, and J. Kulys. Computer simulation of the response of amperometric biosensors in stirred and non stirred solution. *Non-linear Analysis: Modelling and Control*, 8:3–18, 2003.
- [20] J.E. Moreira, S.P. Midkiff, M. Gupta, P.V. Artigas, M. Snir, and R.D. Lawrence. Java programming for high performance numerical computing. *IBM Systems Journal*, 39:21–56, 2000.